Electroweak right-handed neutrinos and new Higgs signals at the LHC

J.L. Díaz-Cruz[a], O. Félix-Beltrán[b], A. Rosado[c] and S. Rosado-Navarro[a]

[a] *Facultad de Ciencias Físico-Matemáticas,*

Benemérita Universidad Autónoma de Puebla,

Apartado Postal 1364, C.P. 72000 Puebla, Pue., México.

[b] *Facultad de Ciencias de la Electrónica,*

Benemérita Universidad Autónoma de Puebla,

Apartado Postal 1152, C.P. 72570 Puebla, Pue., México.

[c] *Instituto de Física, Benemérita Universidad Autónoma de Puebla,*

Apartado Postal J-48, C.P. 72570 Puebla, Pue., México.

(Dated: July 14, 2010)

Abstract

We explore the phenomenology of the Higgs sector in a model that includes right-handed neutrinos, with a mass of the order of the electroweak scale. In this model all scales arise from spontaneous symmetry breaking, thus the Higgs sector includes an extra Higgs singlet, in addition to the standard model Higgs doublet. The scalar spectrum includes two neutral CP-even states (h and H, with $m_h < m_H$) and a neutral CP-odd state (σ) that can be identified as a pseudo-Majoron. The parameter of the Higgs potential are constrained using a perturbativity criteria, which amounts to solve the corresponding RGE. The relevant Higgs BR's and some cross-sections are discussed, with special emphasis on the detection of the invisible Higgs signal at the LHC.

PACS numbers: 12.60.Fr, 14.60.St, 14.80.Ec, 14.80.Va

I. INTRODUCTION.

Neutrino physics has received a tremendous amount of experimental input in the last decade [1–7]. Neutrino oscillations could be considered the first signal of physics beyond the Standard Model (SM) [8], and they suggest that neutrinos are massive. After the data on atmospheric and accelerator neutrino oscillations, we know that there is a non-vanishing mass difference [9]. From solar and reactor neutrino oscillations, we know that at least two neutrinos are not massless [10]. On the theoretical side, the origin of neutrino masses and their observed patterns (for the neutrino mass squared differences) as well as the mixing angles still represent a mystery [11]. There are some ideas that have been widely used in order to explore the situation, like the Zee model [12] or the see-saw mechanism [13, 14] in its several incarnations [15], but we are far from a deep understanding of this issue. Most of the actual realizations of these mechanisms postpone the desired knowledge up to very high, experimentally unaccessible, energy scales. Concretely, since the introduction of Right-handed (RH) neutrinos seem to be the obvious addition needed in order to write a Dirac mass for the neutrinos, most models assume their existence with a mass scale typically of size $\sim 10^{13} - 10^{16}$ GeV (and the seesaw mechanism can be used to explain the smallness of the neutrino mass scale) [14, 15].

In this paper we adhere to the idea that our current (experimental) knowledge of particle physics should be explored by a "truly minimal" extension of the SM. In this tenor we consider the possibility of having only one scale associated with all the high energy physics (HEP) phenomena. Since the SM is consistent with all data so far (modulo neutrino masses), we propose a minimal extension of the SM where new phenomena associated to neutrino physics can also be explained by physics at the Electroweak (EW) scale *i.e.* $O(10)$ GeV to $O(1)$ TeV (similar approaches can be found in [16–19]). Thus, we assume

- SM particle content and gauge interactions.

- Existence of three RH neutrinos with a mass scale of EW size.

- Global $U(1)_L$ spontaneously (and/or explicitly) broken at the EW scale by a single complex scalar field.

- All mass scales come from spontaneous symmetry breaking (SSB). This leads to a Higgs sector that includes a Higgs $SU(2)_L$ doublet field Φ with hypercharge 1 (i.e. the

usual SM Higgs doublet) and a SM singlet complex scalar field η with lepton number -2.

This approach will have an effect on the type of signals usually expected for the SM Higgs sector, where the hierarchy (naturalness) problem resides. By enlarging the SM to explain the neutrino experimental results, we can get a richer spectrum of signals for Higgs physics and it is expected that once the LHC starts, it will test some of the theoretical frameworks created thus far, including ours. Furthermore, in order to fully probe whether the Higgs bosons have "Dirac" and/or "Majorana" couplings, we might have to wait until we reach a "precision Higgs era" at a linear collider [20].

In this work, we explore in detail the Higgs phenomenology that results in this model, with right-handed neutrinos having a mass scale of the order of the electroweak scale. The scalar spectrum includes two neutral CP-even states (h and H with $m_h < m_H$) and a neutral CP-odd state (σ) that can be identified as a pseudo-Majoron. The parameter of the Higgs potential are constrained using a perturbativity criteria, which requires solving the corresponding RGE. We then evaluate the dominant BR's and some cross sections, with special emphasis on the detection of the invisible Higgs signal at the LHC.

Our paper is organized as follows. In section II, we discuss the Lagrangian of our model. In section III, we present the constraints on the model parameters obtained by using the Renormalization Group Equations. In section IV, we give the formulae to calculate the Higgs decays, while in section V, we discuss the possibility of detecting the invisible Higgs signal at the LHC. Finally, in section VI, we summarize our results and present some conclusions.

II. THE MODEL

Taking into account the previous assumptions it is straightforward to write the Lagrangian of the model. The relevant terms for Higgs and neutrino sectors are

$$\mathcal{L}_{\nu H} = \mathcal{L}_{\nu y} - V \ , \tag{1}$$

with

$$\mathcal{L}_{\nu y} = -y_{\alpha i}\overline{L}_\alpha N_{Ri}\Phi - \frac{1}{2}Z_{ij}\eta\overline{N}^c_{Ri}N_{Rj} + h.c. \ , \tag{2}$$

where N_R represents the RH neutrinos, $\psi^c = C\gamma^0\psi^*$ and $\psi^c_R \equiv (\psi_R)^c = P_L\psi^c$ has left-handed chirality. The Yukawa couplings will be adjusted to reproduce the neutrino masses. The

potential of the Higgs sector is given by

$$
\begin{aligned}
V = & \mu_D^2 \Phi^\dagger \Phi + \frac{\lambda}{2} \left(\Phi^\dagger \Phi\right)^2 + \mu_S^2 \eta^* \eta + \lambda' \left(\eta^* \eta\right)^2 \\
& + \kappa \left(\eta \Phi^\dagger \Phi + h.c.\right) + \lambda_m \left(\Phi^\dagger \Phi\right) \left(\eta^* \eta\right) \ .
\end{aligned}
\tag{3}
$$

Note that the fifth term in the potential (proportional to κ) breaks explicitly the U(1) symmetry associated to lepton number. This is going to be relevant when we discuss the features of the Majoron later in the paper.

Assuming that the scalar fields acquire vacuum expectation values (vevs) in such a way that Φ and η are responsible for EW and global U(1)$_L$ symmetry breaking, respectively, we can write the shifted fields (in unitary gauge)

$$
\Phi = \begin{pmatrix} 0 \\ \frac{\phi^0 + v}{\sqrt{2}} \end{pmatrix} \quad \text{and} \quad \eta = \frac{\rho + u + i\sigma}{\sqrt{2}} \ ,
\tag{4}
$$

where $v/\sqrt{2}$ and $u/\sqrt{2}$ are the vevs of Φ and η, respectively. Then, we obtain the following minimization conditions:

$$
\mu_D^2 = -\frac{1}{2} \left(\lambda v^2 + \lambda_m u^2 - 2\sqrt{2}\kappa u\right)
\tag{5}
$$

$$
\mu_S^2 = -\frac{1}{2u} \left(2\lambda' u^3 + \lambda_m u v^2 + \sqrt{2}\kappa v^2\right) \ .
\tag{6}
$$

The form of the mass matrix for the scalar fields is given by

$$
m_S^2 = \begin{pmatrix} \lambda v^2 & vu(\lambda_m - \sqrt{2}r) \\ vu(\lambda_m - \sqrt{2}r) & 2\lambda' u^2 + \frac{1}{\sqrt{2}}rv^2 \end{pmatrix} \ ,
\tag{7}
$$

where $r \equiv -\kappa/u$. The mass for the σ (pseudo-Majoron) field is

$$
m_\sigma^2 = \frac{rv^2}{\sqrt{2}} \ .
\tag{8}
$$

Note that, as expected, m_σ^2 is proportional to the parameter κ associated to the explicit breaking of the U(1)$_L$ symmetry.

We are working under the assumption that the explicit breaking is quite small, i.e. $\kappa <<$ EW scale. This explains why we are minimizing the potential with respect to η, thus assuming it breaks the global symmetry spontaneously. Furthermore we expect the SSB generated by the vev of $\langle\eta\rangle = u/\sqrt{2}$ to be of EW scale size, and so we work under the

4

assumption $r \equiv -\kappa/u << 1$. For example, taking $-\kappa \sim \mathrm{KeV}$ one obtains $r \sim 10^{-9} - 10^{-7}$, which then leads to a Majoron mass of $O(10)$ MeV.

From Eq.(7), we can obtain the mass eigenstates

$$\mathcal{H} = \begin{pmatrix} \phi^0 \\ \rho \end{pmatrix} = \begin{pmatrix} \cos\alpha & -\sin\alpha \\ \sin\alpha & \cos\alpha \end{pmatrix} \begin{pmatrix} h \\ H \end{pmatrix} . \tag{9}$$

Using these definitions to rewrite the Yukawa Lagrangian (Eq.(2)), we obtain

$$\begin{aligned}
\mathcal{L}_{\nu y} \supset & -y_{\alpha i}\overline{\nu}_{L\alpha}N_{Ri}\frac{\phi^0}{\sqrt{2}} - \frac{1}{2}Z_{ij}\frac{(\rho + i\sigma)}{\sqrt{2}}\overline{N}^c_{Ri}N_{Rj} + h.c. \\
= & \left(-\frac{y_{\alpha i}}{\sqrt{2}}\overline{\nu}_{L\alpha}N_{Ri}(c_\alpha\, h - s_\alpha\, H) + h.c. \right) - \left(\frac{i}{2\sqrt{2}}Z_{ij}\overline{N}^c_{Ri}N_{Rj}\sigma + h.c. \right) \\
& - \left(\frac{1}{2\sqrt{2}}Z_{ij}\overline{N}^c_{Ri}N_{Rj}(s_\alpha\, h + c_\alpha\, H) + h.c \right) .
\end{aligned} \tag{10}$$

We now make some comments regarding neutrino mass scales. Since we are interested in RH neutrinos at the EW scale, we take their masses to be in that scale, i.e. anywhere from a few to hundreds of GeV. The Dirac part on the other hand will be constrained from the implementation of the seesaw mechanism. The neutrino mass matrix is given by

$$m_\nu = \begin{pmatrix} 0 & m_D \\ m_D & m_M \end{pmatrix} , \tag{11}$$

where $(m_D)_{\alpha i} = y_{\alpha i}v/\sqrt{2}$. This is a 6×6 matrix, difficult to analyze in general. But as an example, let us consider the third family of SM fields and one RH neutrino, thus Eq.(11) becomes a 2×2 matrix. Assuming $m_D << m_M$ we obtain the eigenvalues $m_1 = -m_D^2/m_M$ and $m_2 = m_M$; then by requiring $m_1 \sim \mathrm{O(eV)}$, $m_2 \sim (10-100)$ GeV, and using $v = 246$ GeV, we obtain an upper bound estimate for the Yukawa coupling $y_{\tau i} \leq 10^{-6}$.

The neutrino mass eigenstates are denoted by ν_1 and ν_2 and are defined such that

$$\begin{aligned}
\nu_\tau &= \cos\theta\, \nu_{L1} + \sin\theta\, \nu_{R2} \\
N &= -\sin\theta\, \nu_{L1} + \cos\theta\, \nu_{R2} ,
\end{aligned} \tag{12}$$

where $\theta = \sqrt{m_D/m_2} \sim 10^{-6} - 10^{-5}$.

The relevant terms in the Lagrangian become

$$\begin{aligned}
\mathcal{L} \supset & \left[h\overline{\nu}^c_{L1}\nu_{L1}\left(-\frac{Z}{2\sqrt{2}}s_\theta^2 s_\alpha \right) + h\overline{\nu}^c_{R2}\nu_{R2}\left(-\frac{Z}{2\sqrt{2}}c_\theta^2 s_\alpha \right) + h.c. \right] \\
& + h\overline{\nu}_{L1}\nu_{R2}\left(\frac{y_\nu}{\sqrt{2}}(s_\theta^2 - c_\theta^2)c_\alpha \right) + h\overline{\nu}_{R2}\nu_{L1}\left(\frac{y_\nu}{\sqrt{2}}(s_\theta^2 - c_\theta^2)c_\alpha \right) ,
\end{aligned} \tag{13}$$

5

where $y_\nu^* = y_\nu$ and $Z \equiv Z_{11}$.

As discussed in the introduction we are also interested in exploring the Higgs decay mode involving the Majoron. Then, we need to rewrite to the terms in the potential that contain the Majoron-Higgs bosons couplings, in terms of mass eigenstates. We obtain:

$$
\begin{aligned}
V \supset & \frac{1}{2}(c_\alpha v\lambda_m + 2s_\alpha u\lambda')h\sigma\sigma - \frac{1}{2}(s_\alpha v\lambda_m - 2c_\alpha u\lambda')H\sigma\sigma \\
& + \frac{1}{4}(c_\alpha^2\lambda_m + 2s_\alpha^2\lambda')hh\sigma\sigma - \frac{1}{2}c_\alpha s_\alpha(\lambda_m - 2\lambda')Hh\sigma\sigma \\
& + \frac{1}{4}(s_\alpha^2\lambda_m + 2c_\alpha^2\lambda')HH\sigma\sigma
\end{aligned}
\tag{14}
$$

III. CONSTRAINTS ON THE MODEL PARAMETERS USING RGE

The parameters that appear in the Higgs potential are essentially unconstrained by any phenomenology argument, therefore we have to resort to some theoretical argument. Here we shall rely on the perturbativity criteria, namely we shall require that any choice of the Higgs parameters (λ_i) at low-energies, which determine the Higgs spectrum and couplings, must remain below 4π when evolve from m_Z up to a high-energy scale (such as M_{GUT} or M_{Planck}).

The corresponding Renormalization Group Equations have been discussed in a slightly different context in [23, 24]. They are given by

$$
\begin{aligned}
\frac{dg_s}{dt} &= \frac{g_s^3}{16\pi^2}[-11 + \frac{4}{3}n_g] \\
\frac{dg}{dt} &= \frac{g^3}{16\pi^2}[-\frac{22}{3} + \frac{4}{3}n_g + \frac{1}{6}] \\
\frac{dg'}{dt} &= \frac{g'^3}{16\pi^2}[A^{YY}] \\
\frac{dy_t}{dt} &= \frac{y_t}{16\pi^2}[\frac{9}{2}y_t^2 - 8g_s^2 - \frac{9}{4}g^2 - \frac{17}{2}g'^2] \\
\frac{dy_i^M}{dt} &= \frac{y_i^M}{16\pi^2}(4(y_i^M)^2 + 2Tr[(y^M)^2]), \quad (i = 1, 2, 3) \\
\frac{d\lambda_1}{dt} &= \frac{1}{16\pi^2}(24\lambda_1^2 + \lambda_3^2 - 6y_t^4 + \frac{9}{8}g^4 + \frac{3}{8}g'^4 + \frac{3}{4}g^2g'^2 + 12\lambda_1 y_t^2 - 9\lambda_1 g^2 - 3\lambda_1 g'^2) \\
\frac{d\lambda_2}{dt} &= \frac{1}{16\pi^2}(20\lambda_2^2 + 2\lambda_3^2 - Tr[(y^M)^4] + 8\lambda_2 Tr[(y^M)^2] \\
\frac{d\lambda_3}{dt} &= \frac{\lambda_3}{16\pi^2}(12\lambda_1 + 8\lambda_2 + 4\lambda_3 + 6y_t^2 - \frac{9}{2}g^2 - \frac{3}{2}g'^2 + 4Tr[(y^M)^2])
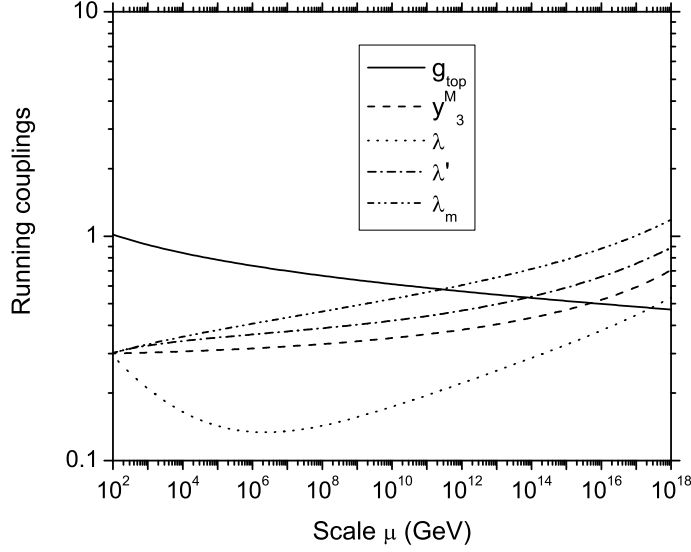\end{aligned}
$$

FIG. 1: Evolution of the running couplings: g_{top}, y_3^M, λ, λ' and λ_m as functions of the scale μ, by taking $g_{top}(100\,\text{GeV}) \approx 1$, and $y_3^M(100\,\text{GeV}) = \lambda(100\,\text{GeV}) = \lambda'(100\,\text{GeV}) = \lambda_m(100\,\text{GeV}) = 0.3$.

where n_g stands by the family number (we are taking $n_g = 3$) and $y^M \equiv diag(y_1^M, y_2^M, y_3^M)$.

We have explored the values of parameters λ, λ', λ_m, which satisfy the perturbative constraint $g_i(M_{GUT})$, $\lambda_i(M_{GUT}) < 4\pi$, and we identify some scenarios that are safe to be studied in the following sections. Namely, we identify the following examples:

1. For $g_{top}(100\,\text{GeV}) \approx 1$, and $y_3^M(100\,\text{GeV}) = \lambda(100\,\text{GeV}) = \lambda'(100\,\text{GeV}) = \lambda_m(100\,\text{GeV}) = 0.3$, (Set 1), we can see from Fig. 1 that their evolution from the EW scale (100 GeV) remains perturbative.

2. On the other hand, for another set of parameters, $g_{top}(100\,\text{GeV}) \approx 1$, and $y_3^M(100\,\text{GeV}) = \lambda(100\,\text{GeV}) = \lambda'(100\,\text{GeV}) = \lambda_m(100\,\text{GeV}) = 0.4$ (Set 2), we find that the couplings blow up at an scale of $O(10^{12})$, as it is shown in Fig. 2. Thus, just by going from 0.3 to 0.4, for the values of the parameters, we find a change of regime.

In what follows, we shall use Set 1 for the parameters of the Higgs potential. This scenario can be taken as an example where parameters have the maximal values allowed by the perturbativity criteria. Lower values are thus allowed too.
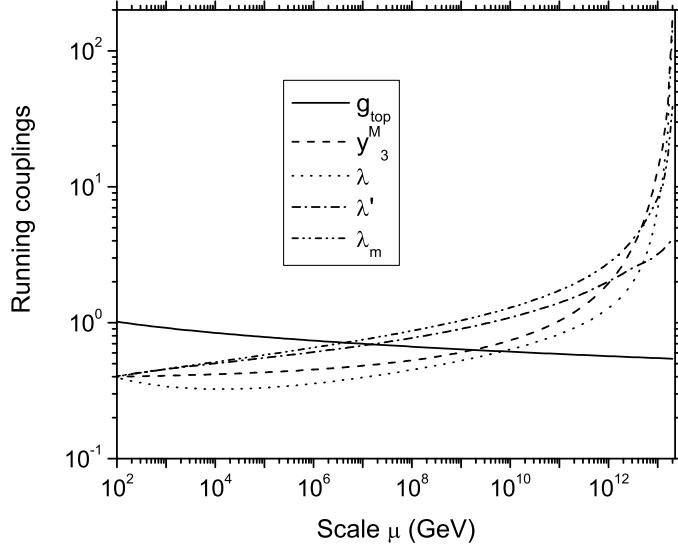
FIG. 2: Evolution of the running couplings: g_{top}, y_3^M, λ, λ' and λ_m as functions of the scale μ, by taking $g_{top}(100\,\text{GeV}) \approx 1$, and $y_3^M(100\,\text{GeV}) = \lambda(100\,\text{GeV}) = \lambda'(100\,\text{GeV}) = \lambda_m(100\,\text{GeV}) = 0.4$.

IV.   HIGGS DECAYS

We are interested now in studying the new Higgs modes that appear in this model. We have evaluated the Higgs decays using the formulae presented in [21], with appropriate modifications to include the changes in couplings due to Higgs mixing. The decay width for the Higgs decay mode into a pair of majorons is given as follows:

$$\Gamma(h \to \sigma\sigma) = \frac{S|c_{h\sigma\sigma}|^2 \sqrt{m_h^4 - 4m_h^2 m_\sigma^2}}{16\pi m_h^3}, \tag{15}$$

where $c_{h\sigma\sigma}$ stands for the coupling $h\sigma\sigma$; which was studied in the Section II. Namely $c_{h\sigma\sigma} = -\frac{i}{2}(c_\alpha v \lambda_m + 2s_\alpha u \lambda')$, $c_{H\sigma\sigma} = \frac{i}{2}(s_\alpha v \lambda_m - 2c_\alpha u \lambda')$. Furthermore, in this case $S = \frac{1}{2!}$.

In Ref. [16] we discussed the Higgs decays to neutrinos and their signatures in this model. The possible relation to Majoron Dark Matter has been considered in Ref. [22].

Here, using Eq. (13) one obtains the following decay widths [26]:

$$\Gamma(h \to \overline{\nu}_1 \nu_1) = \frac{m_h}{64\pi}|Z|^2 s_\theta^4 s_\alpha^2 , \tag{16}$$

$$\Gamma(h \to \overline{\nu}_2 \nu_2) = \frac{m_h}{64\pi}|Z|^2 c_\theta^4 s_\alpha^2 \left(1 - \frac{4m_2^2}{m_h^2}\right)^{3/2} , \tag{17}$$

8

$$\Gamma(h \to \overline{\nu}_1 \nu_2) \;=\; \frac{m_h}{16\pi} y_\nu^2 (s_\theta^2 - c_\theta^2)^2 c_\alpha^2 \left(1 - \frac{m_2^2}{m_h^2} \right)^2 . \tag{18}$$

In order to perform our numerical analysis, we shall take values allowed by the perturbative analysis (Set 1) for the parameters λ_m, λ', and some values for the vev u and $\cos\alpha$. The mass of the Majoron m_σ is given in terms of the parameter u as follows:

$$m_\sigma(u = 10\,\mathrm{GeV}) \approx 65\,\mathrm{MeV},$$

$$m_\sigma(u = 246\,\mathrm{GeV}) \approx 13\,\mathrm{MeV}$$

For the light Higgs boson (h) we compute the BR's of the different decay modes in the mass range $100 \leq m_h \leq 200$ GeV, assuming that the heavier Higgs boson has a mass above 200 GeV, while the Majoron has a mass of the order tenths of MeV.

In Figs. 3-6 we present our results for the decays: $h \to b\overline{b}$, $h \to \tau\overline{\tau}$, $h \to W^+W^-$, $h \to Z^0 Z^0$, $h \to \nu_2\nu_2$, and $h \to \sigma\sigma$, which are the most important two body decay modes. In Fig. 3 we show the corresponding BR's considering $m_\sigma = 13\,\mathrm{MeV}$ with $\lambda' = \lambda_m = 0.1$. Figs. 3(a), 3(b) and 3(c), corresponds to $\cos\alpha = 0.1$, 0.5, ≈ 1, respectively. We can see that $BR(h \to \nu_2\nu_2)$ is dominant for $\cos\alpha = 0.1$, 0.5, but it is of $O(10^{-7})$ for $\cos\alpha \approx 1$. On the other hand, the $BR(h \to \sigma\sigma)$ is relevant for any value of $\cos\alpha$, with a value of $O(10^{-2} - 10^{-1})$ and becoming dominant when $\cos\alpha \approx 1$, in the Higgs mass range $100 \lesssim m_h \lesssim 160\,\mathrm{GeV}$. We can see a similar behavior in Fig. 4, where we are considering $m_\sigma = 65\,\mathrm{MeV}$. The $BR(h \to \nu_2\nu_2)$ is of the same order of magnitude for a given value of $\cos\alpha$, and this quantity is independent of the value of m_σ. On the other side, we observe in these figures, that $BR(h \to \sigma\sigma)$ is sensitive to the value of m_σ; when $m_\sigma = 65\,\mathrm{MeV}$, this BR drops to $O(10^{-4})(O(10^{-3}))$ for $\cos\alpha = 0.1(\cos\alpha = 0.5)$. But it is still dominant for $\cos\alpha \approx 1$ in the mass range $100 \lesssim m_h \lesssim 160\,\mathrm{GeV}$.

When we consider $\lambda' = \lambda_m = 0.3$ (see Figs. 5-6), the $BR(h \to \nu_2\nu_2)$ has the same behavior as in the scenario with $\lambda' = \lambda_m = 0.1$. However, in this case the $BR(h \to \sigma\sigma)$ has an enhancement, becoming of $O(10^{-1})$ for $\cos\alpha = 0.1, 0.5$ and $m_\sigma = 13\,\mathrm{MeV}$, but it is again dominant for $\cos\alpha \approx 1$, reaching values of $O(10^{-1})$ for $100 \lesssim m_h \lesssim 160\,\mathrm{GeV}$. On the other hand, the $BR(h \to \nu_2\nu_2)$ in no longer dominant for $m_h \sim 100\,\mathrm{GeV}$ when $m_\sigma = 13\,\mathrm{MeV}$ and $\cos\alpha = 0.1$, 0.5. In the case when $m_\sigma = 65\,\mathrm{MeV}$, $BR(h \to \sigma\sigma)$ has $O(10^{-3})$ $(O(10^{-2}))$ for $\cos\alpha = 0.1$ $(\cos\alpha = 0.5)$ and, again, it is dominant in the case with $\cos\alpha \approx 1$ for $100 \lesssim m_h \lesssim 160\,\mathrm{GeV}$. If we compare these BR's with the corresponding decay mode $h \to$

WW. We can see in Figs. 3-6 that the $BR(h \to WW)$ is sensitive to the value of $\cos \alpha$, but not to the value of m_σ. It is also shown in these figures that the decay mode to WW has a BR of $O(10^{-3})$ for $\cos \alpha = 0.1$, and $O(10^{-2})$ for $\cos \alpha = 0.5$, and it becomes dominant when $\cos \alpha \approx 1$, for any value of m_σ, and $160 \lesssim m_h < 200\,\text{GeV}$. This behavior is realized for both $\lambda' = \lambda_m = 0.1$ and 0.3.

On the other hand, for the heavy Higgs boson (H) we consider the mass range $150 \leq m_H \leq 500$, fixing the light Higgs boson mass with two values $m_h = 114$ GeV and $m_h = 160$ GeV.

In Figs. 7-10 we present our results for the decays: $H \to b\bar{b}$, $H \to \tau\bar{\tau}$, $H \to W^+W^-$, $H \to Z^0 Z^0$, $H \to \nu_2 \nu_2$, and $H \to \sigma\sigma$, which are the most important two body decay modes. In Fig. 7 we show the BR's considering $m_\sigma = 13\,\text{MeV}$ and $\lambda' = \lambda_m = 0.1$. Figs. 7(a), 7(b) and 7(c), corresponds to $\cos \alpha = 0.1$, 0.5, ≈ 1, respectively. We can see that the $BR(h \to \nu_2 \nu_2)$ is dominant for $\cos \alpha = 0.1$, and it is no longer dominant when $m_H \gtrsim 250$ GeV for $\cos \alpha = 0.5$, and it is of $O(10^{-7})$ for $\cos \alpha \approx 1$. On the other hand, $BR(H \to \sigma\sigma)$ is relevant for any value of $\cos \alpha$ and its relevance is larger when $\cos \alpha \approx 1$. We can see a similar behavior for $BR(H \to \nu_2 \nu_2)$ and $BR(H \to \sigma\sigma)$ in Fig. 8, where we have considered $m_\sigma = 65\,\text{MeV}$. The $BR(H \to \nu_2 \nu_2)$ is the dominant mode, when $\cos \alpha = 0.1$ independently of m_σ. The most important decay mode is $BR(H \to \sigma\sigma)$, when $\cos \alpha \approx 1$ and it does not dependent on the m_σ value.

When we consider $\lambda' = \lambda_m = 0.3$ (see Figs. 9 and 10), the $BR(h \to \sigma\sigma)$ shows an enhancement with respect to the value shown in the previous case, where we are taking $\lambda' = \lambda_m = 0.1$. We can see in Figs. 9 and 10, a similar behavior for $BR(H \to \nu_2 \nu_2)$ and $BR(H \to WW)$, when we consider $m_\sigma = 13\,\text{MeV}$ and $m_\sigma = 65\,\text{MeV}$. Namely, the $BR(H \to \nu_2 \nu_2)$ is the dominant one, when $\cos \alpha = 0.1$ independently of m_σ. The most important decay mode is $BR(H \to \sigma\sigma)$, when $\cos \alpha \approx 1$ and it does not dependent on the m_σ value. This behavior is realized for $\lambda' = \lambda_m = 0.1$, 0.3

V. DETECTION AT LHC

We are also interested in determining whether the invisible Higgs decay could be observed at LHC. We shall use the results of Ref. [25], where a detailed study of detectability of an invisible Higgs was performed. These authors consider the production mechanisms $pp \to$

	Minimal value of R to be observed at the LHC		
Luminosity	$m_h = 120\,\text{GeV}$	$m_h = 140\,\text{GeV}$	$m_h = 160\,\text{GeV}$
30 fb^{-1}	0.404 (0.439)	0.550 (0.598)	0.739 (0.803)
50 fb^{-1}	0.313 (0.340)	0.426 (0.463)	0.573 (0.622)
100 fb^{-1}	0.221 (0.241)	0.301 (0.328)	0.405 (0.440)

TABLE I: Minimal value of the parameter R for an event $h \to inv.$ to be observed with a significance of $4\,\sigma$ at the LHC, with an integrated Luminosity $\mathcal{L}$, as a function of the Higgs boson mass m_h. Here we take the cut on $\not{p}_T = 75$ GeV of Ref. [25]. The numbers in parentheses include the estimated $Z + jets$ background discussed in Ref. [25]

hZ^0, for the signal, as well as $pp \to W^+W^- \to h$ and $pp \to h + jet$. Here, we shall use for illustration purposes, the associated production with $Z^0 + h(\to inv.)$; a detailed set of cuts is proposed in order to determine the backgrounds [25]. Their analysis can be used to determine the minimum value of the ratio

$$R = \frac{g^2_{\phi ZZ}}{g^2_{\phi_{SM} ZZ}} \times BR(h \to \sigma\sigma) \tag{19}$$

that can produce a 4σ signal. This is shown in Table I for two different values of the Luminosity $\mathcal{L}$ and some values of m_h. We display in Table II, the value of R for several choices of parameters within our model, and it can be seen that these choices are consistent with the perturbative analysis of the previous section. For instance, for $\lambda' = \lambda_m = 0.3$, and taking $\cos\alpha = 0.99$, $u = 246$ GeV and $m_H = 160$, we obtain $R = 0.846$. This means that it coul be possible to find evidence of the existence of a pseudo-Majoron through an invisible Higgs at the LHC for this scenario, with a significance of $4\,\sigma$, even with an integrated Luminosity of $\mathcal{L} = 30\,\text{fb}^{-1}$.

VI. CONCLUSIONS

We have explored in detail the Higgs phenomenology that results in a model where right-handed neutrinos have a mass scale of the order of the electroweak scale. In this model all scales arise from spontaneous symmetry breaking, and this is achieved with a Higgs sector that includes an extra Higgs singlet in addition to the standard model Higgs doublet. The

$\cos\alpha$	u	$R = (g_{\phi ZZ}^2/g_{\phi_{SM}ZZ}^2) \times BR(h \to inv.)$		
		$m_h = 120\,\mathrm{GeV}$	$m_h = 140\,\mathrm{GeV}$	$m_h = 160\,\mathrm{GeV}$
0.9	$10\,\mathrm{GeV}$	0.378	0.315	0.264
0.9	$246\,\mathrm{GeV}$	0.615	0.563	0.514
0.95	$10\,\mathrm{GeV}$	0.578	0.510	0.448
0.95	$246\,\mathrm{GeV}$	0.743	0.697	0.650
0.99	$10\,\mathrm{GeV}$	0.858	0.820	0.780
0.99	$246\,\mathrm{GeV}$	0.901	0.874	0.846

TABLE II: Value of R for the process $h \to \sigma\sigma$, by fixing $\lambda' = \lambda_m = 0.3$ and by taking several values of the parameters $u = \sqrt{2}\,\langle\eta\rangle$ and $\cos\alpha$, as a function of the Higgs boson mass m_h.

scalar spectrum includes two neutral CP-even states (h and H with $m_h < m_H$) and a neutral CP-odd state (σ) that can be identified as a pseudo-Majoron.

The parameters that appear in the Higgs potential are essentially unconstrained by any phenomenology argument, therefore we have to resorted to some theoretical argument. Here we have relied on the perturbativity criteria, namely we have required that any choice of Higgs parameters at low-energies, which determine the Higgs spectrum and couplings, must remain below 4π when evolve from m_Z up to a high-energy scale (such as M_{GUT} or M_{Planck}).

Thus, we have explored the values of parameters λ, λ', λ_m, which satisfy the perturbative constraint $g_i(M_{GUT})$, $\lambda_i(M_{GUT}) < 4\pi$, and we have identified some safe scenarios that are studied in this paper.

We have concluded that Set 1 ($g_{top}(100\,\mathrm{GeV}) \approx 1$, and $y_3^M(100\,\mathrm{GeV}) = \lambda(100\,\mathrm{GeV}) = \lambda'(100\,\mathrm{GeV}) = \lambda_m(100\,\mathrm{GeV}) = 0.3$) can be taken as a scenario for the parameters of the Higgs potential having the maximal values allowed by the perturbative analysis.

The relevant Higgs BR and cross-sections are discussed, with special emphasis on the detection of the invisible Higgs signal at the LHC. We conclude that it could be possible to detect evidence of the existence of a pseudo-Majoron σ through an invisible Higgs signal at the LHC for some values of parameters.

for financial support.

[1] Q. R. Ahmad *et al.* [SNO Collaboration], Phys. Rev. Lett. **89**, 011301 (2002) [arXiv:nucl-ex/0204008].

[2] C. K. Jung, C. McGrew, T. Kajita and T. Mann, Ann. Rev. Nucl. Part. Sci. **51**, 451 (2001).

[3] K. Eguchi *et al.* [KamLAND Collaboration], Phys. Rev. Lett. **90**, 021802 (2003) [arXiv:hep-ex/0212021].

[4] M. H. Ahn *et al.* [K2K Collaboration], Phys. Rev. Lett. **90**, 041801 (2003) [arXiv:hep-ex/0212007].

[5] T. Schwetz, Phys. Scripta **T127**, 1 (2006) [arXiv:hep-ph/0606060].

[6] M. Maltoni, T. Schwetz, M. A. Tortola and J. W. F. Valle, New J. Phys. **6**, 122 (2004) [arXiv:hep-ph/0405172].

[7] G. L. Fogli *et al.*, Phys. Rev. D **75**, 053001 (2007) [arXiv:hep-ph/0608060].

[8] S. L. Glashow, Nucl. Phys. **22**, 579 (1961); S. Weinberg, Phys. Rev. Lett. **19**, 1264 (1967); A. Salam, Proc. 8th NOBEL Symposium, ed. N. Svartholm (Almqvist and Wiksell, Stockholm, 1968), p. 367.

[9] Y. Fukuda *et al.* [Super-Kamiokande Collaboration], Phys. Rev. Lett. **81**, 1158 (1998) [Erratum-ibid. **81**, 4279 (1998)] [arXiv:hep-ex/9805021].

[10] D. G. Michael *et al.* [MINOS Collaboration], Phys. Rev. Lett. **97**, 191801 (2006) [arXiv:hep-ex/0607088]; S. Abe *et al.* [KamLAND Collaboration], Phys. Rev. Lett. **100**, 221803 (2008) [arXiv:0801.4589 [hep-ex]].

[11] For a review see: J. W. F. Valle, J. Phys. Conf. Ser. **53**, 473 (2006) [arXiv:hep-ph/0608101].

[12] A. Zee, Phys. Lett. B **93**, 389 (1980) [Erratum-ibid. B **95**, 461 (1980)].

[13] P. Minkowski, Phys. Lett. B **67**, 421 (1977).

[14] M. Gell-Mann, P. Ramond and R. Slansky, Proceedings of the Supergravity Stony Brook Workshop, New York 1979, eds. P. Van Nieuwenhuizen and D. Freedman; T. Yanagida, Proceedings of the Workshop on Unified Theories and Baryon Number in the Universe, Tsukuba, Japan 1979, eds. A. Sawada and A. Sugamoto; R. N. Mohapatra and G. Senjanovic, Phys. Rev. Lett. **44**, 912 (1980).

[15] J. Schechter and J. W. F. Valle, Phys. Rev. D **22**, 2227 (1980).

[16] A. Aranda, O. Blanno and J. Lorenzo Diaz-Cruz, Phys. Lett. B **660**, 62 (2008) [arXiv:0707.3662 [hep-ph]].

[17] P. Q. Hung, Phys. Lett. B **649**, 275 (2007) [arXiv:hep-ph/0612004].

[18] M. L. Graesser, arXiv:0705.2190 [hep-ph].

[19] A. de Gouvea, arXiv:0706.1732 [hep-ph].

[20] E. Accomando *et al.* [CLIC Physics Working Group], arXiv:hep-ph/0412251.

[21] J. Gunion, H. Haber, G. Kane and S. Dawson, *The Higgs Hunter's Guide*, Addison-Wesley Publishig Company, Reading, MA, 1990.

[22] A. Aranda and F. J. de Anda, Phys. Lett. B **683**, 183 (2010) [arXiv:0909.2667 [hep-ph]].

[23] L. Basso, S. Moretti and G. M. Pruna, arXiv:1004.3039 [hep-ph].

[24] L. Basso, *A minimal extension of the Standard Model with B-L gauge symmetry*, (Master Thesis, Universitá degli Studi di Padova, 2007), at http://www.hep.phys.soton.ac.uk/∼l.basso/B-L Master Thesis.pdf.

[25] H. Davoudiasl, T. Han and H. E. Logan, Phys. Rev. D **71**, 115007 (2005) [arXiv:hep-ph/0412269].

[26] All SM decay widths will include an extra factor of c_α^2
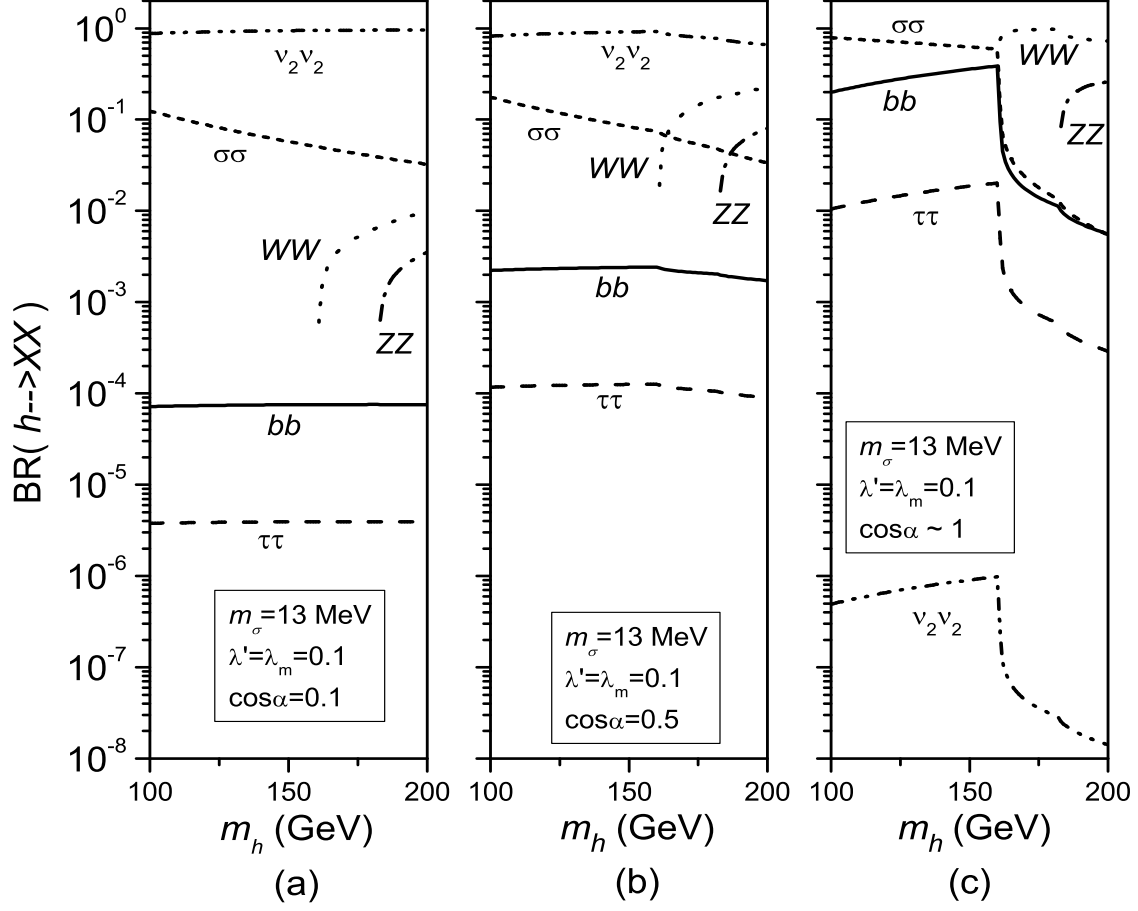
FIG. 3: Braching ratios for the decay $h \to XX$ with $m_\sigma = 13\,\text{MeV}$, $\lambda' = \lambda_m = 0.1$ and three different values for $\cos\alpha$: (a) $\cos\alpha = 0.1$, (b) $\cos\alpha = 0.5$ and (c) $\cos\alpha \approx 1$.
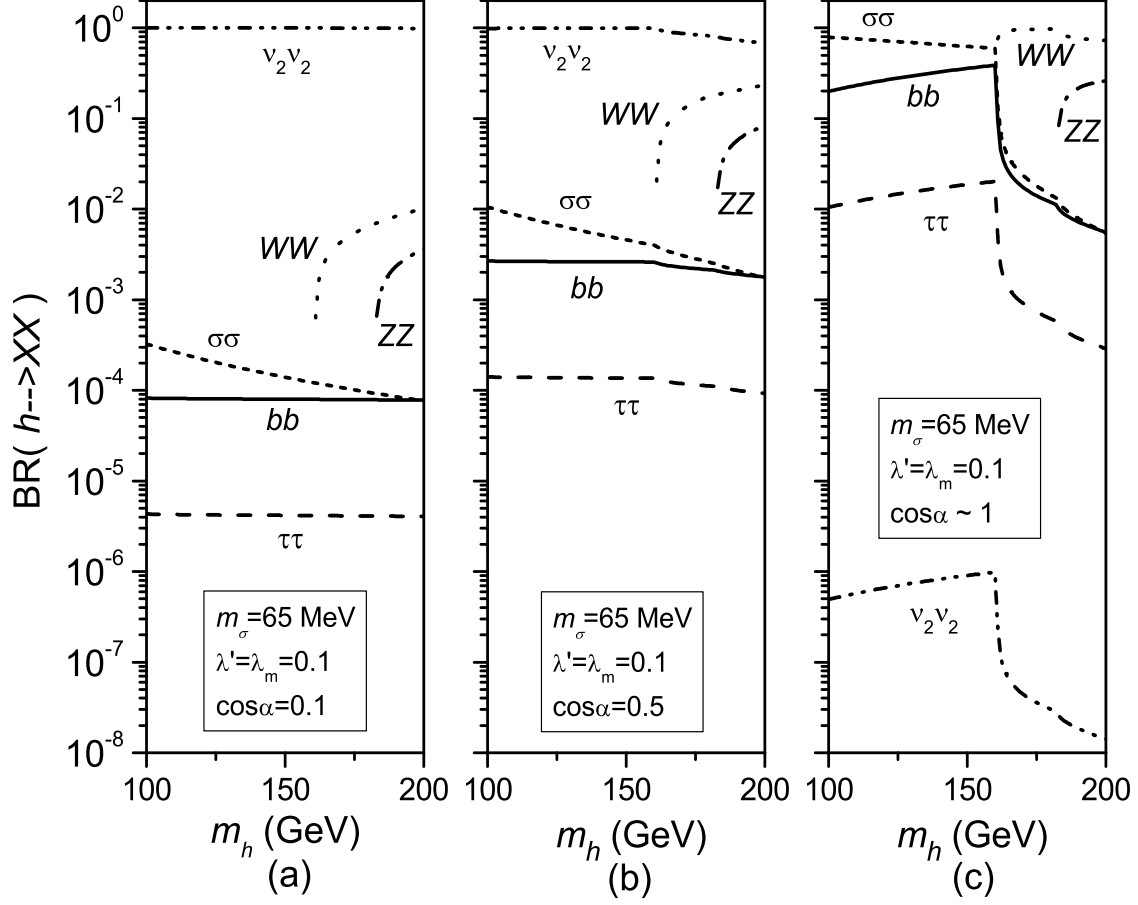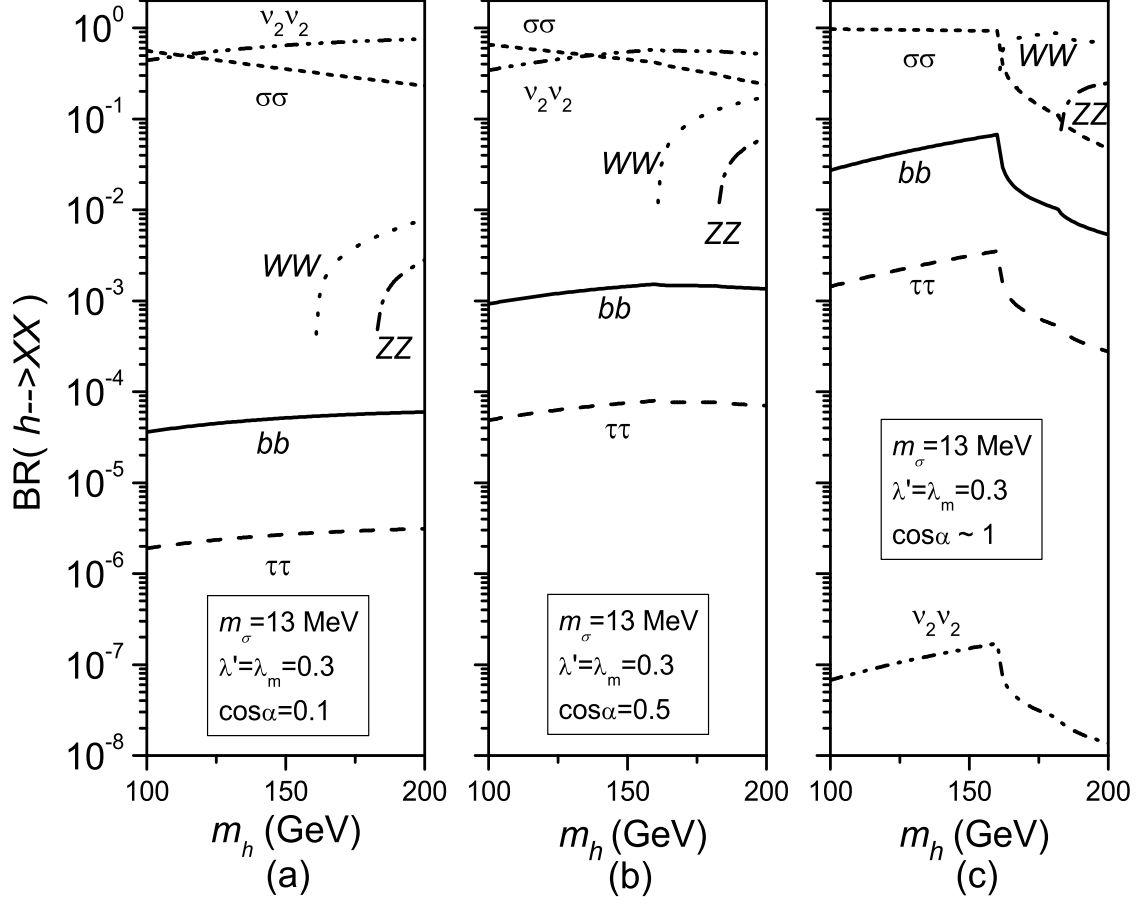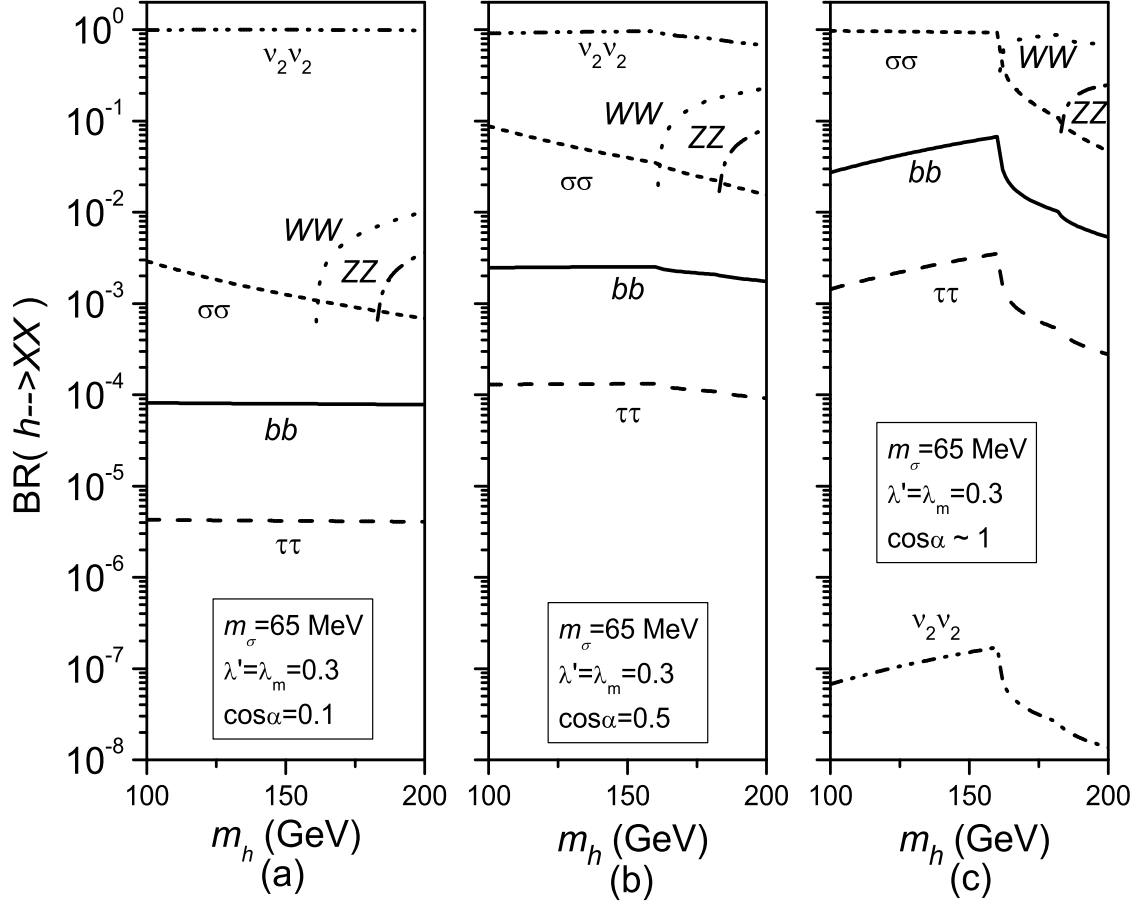
FIG. 4: Braching ratios for the decay $h \rightarrow XX$ with $m_\sigma = 65 \, \text{MeV}$, $\lambda' = \lambda_m = 0.1$ and three different values for $\cos \alpha$: (a) $\cos \alpha = 0.1$, (b) $\cos \alpha = 0.5$ and (c) $\cos \alpha \approx 1$.
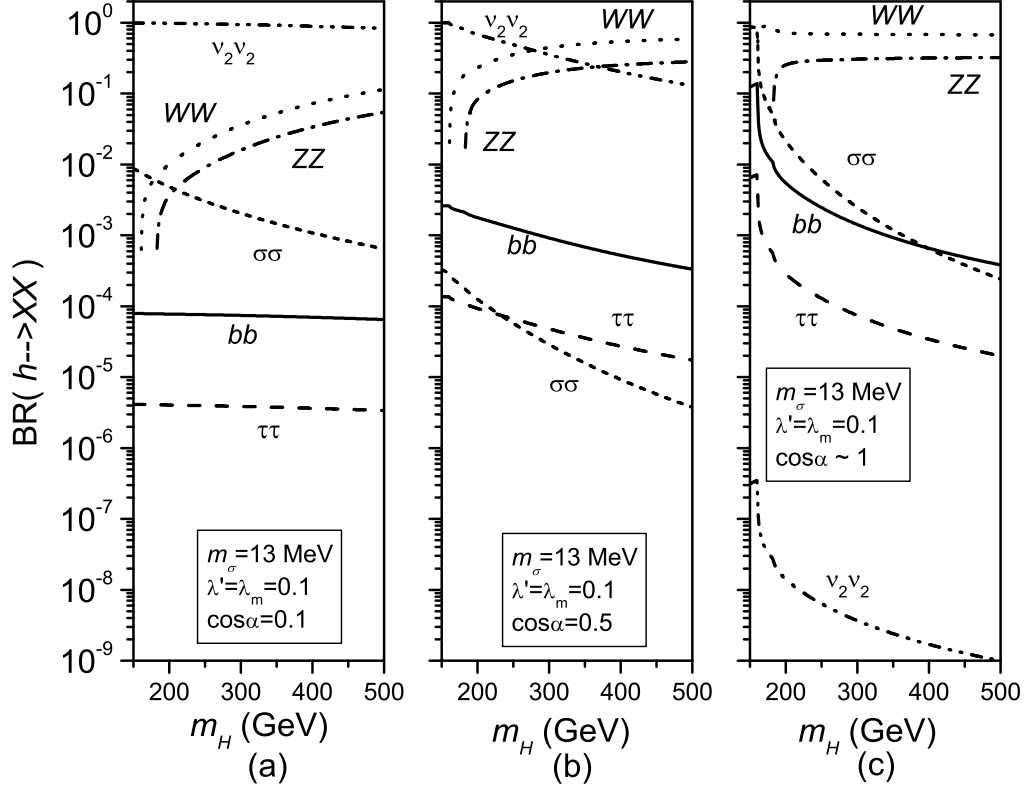
FIG. 5: Braching ratios for the decay $h \to XX$ with $m_\sigma = 13\,\mathrm{MeV}$, $\lambda' = \lambda_m = 0.3$ and three different values for $\cos\alpha$: (a) $\cos\alpha = 0.1$, (b) $\cos\alpha = 0.5$ and (c) $\cos\alpha \approx 1$.

FIG. 6: Braching ratios for the decay $h \to XX$ with $m_\sigma = 65 \, \text{MeV}$, $\lambda' = \lambda_m = 0.3$ and three different values for $\cos\alpha$: (a) $\cos\alpha = 0.1$, (b) $\cos\alpha = 0.5$ and (c) $\cos\alpha \approx 1$.
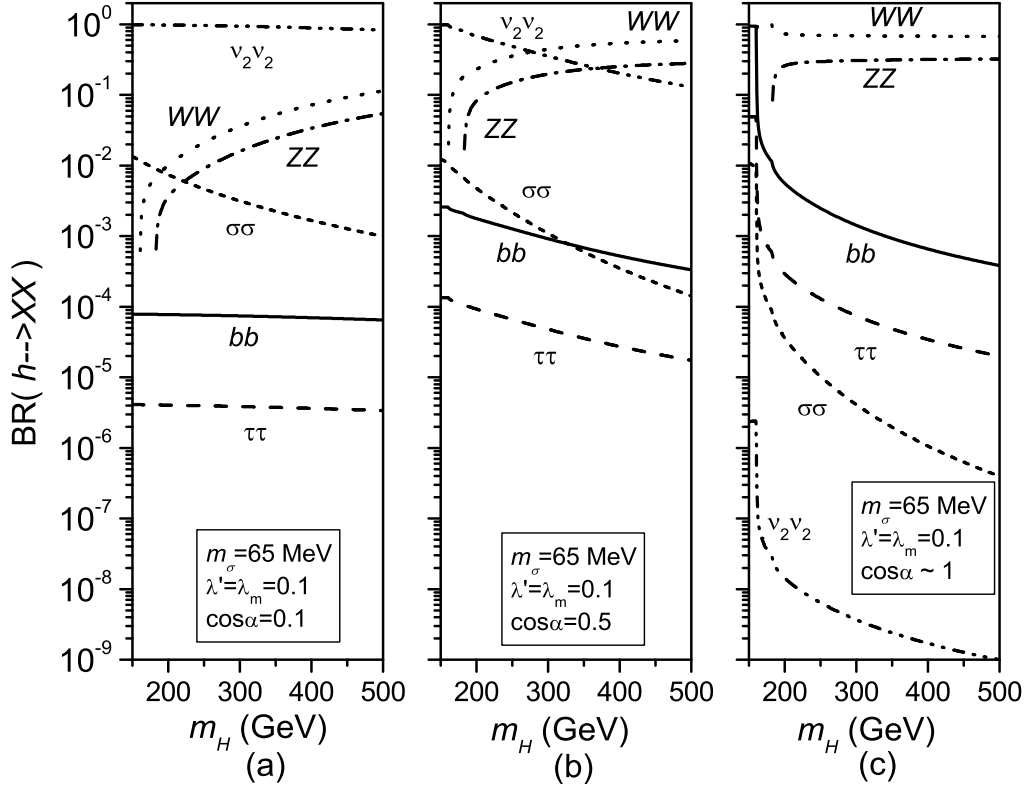
FIG. 7: Braching ratios for the decay $H \to XX$ with $m_\sigma = 13\,\text{MeV}$, $\lambda' = \lambda_m = 0.1$ and three different values for $\cos\alpha$: (a) $\cos\alpha = 0.1$, (b) $\cos\alpha = 0.5$ and (c) $\cos\alpha \approx 1$.

FIG. 8: Braching ratios for the decay $H \to XX$ with $m_\sigma = 65\,\mathrm{MeV}$, $\lambda' = \lambda_m = 0.1$ and three different values for $\cos\alpha$: (a) $\cos\alpha = 0.1$, (b) $\cos\alpha = 0.5$ and (c) $\cos\alpha \approx 1$.
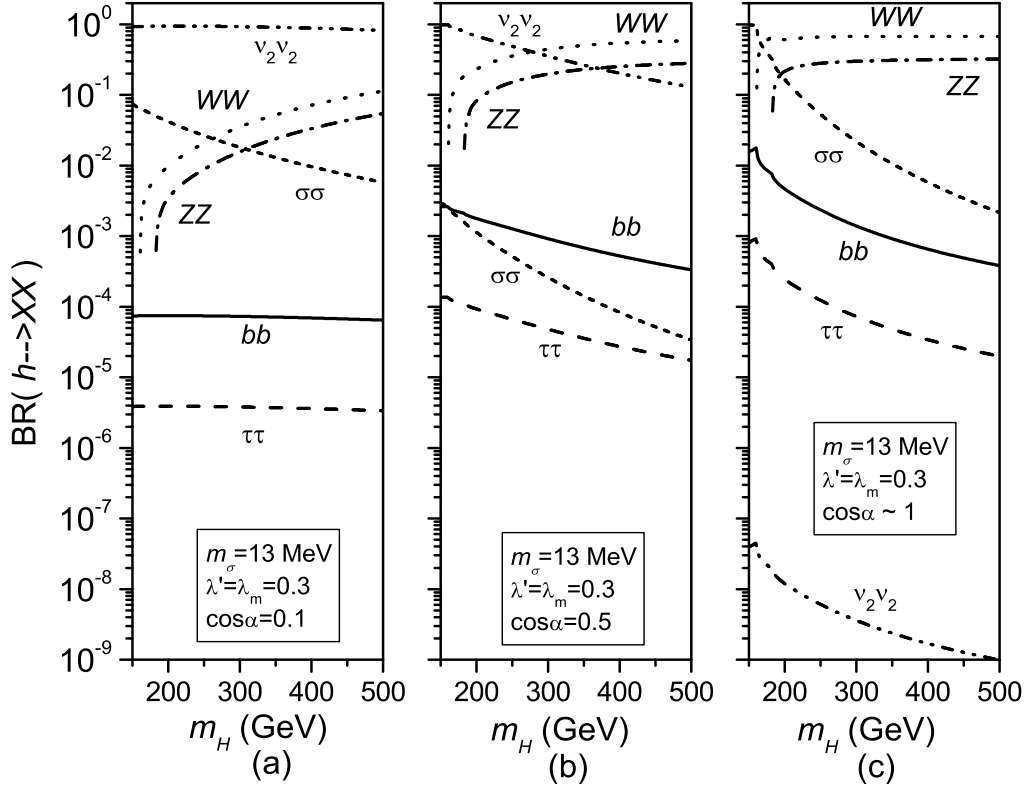
FIG. 9: Braching ratios for the decay $H \rightarrow XX$ with $m_\sigma = 13\,\mathrm{MeV}$, $\lambda' = \lambda_m = 0.3$ and three different values for $\cos\alpha$: (a) $\cos\alpha = 0.1$, (b) $\cos\alpha = 0.5$ and (c) $\cos\alpha \approx 1$.
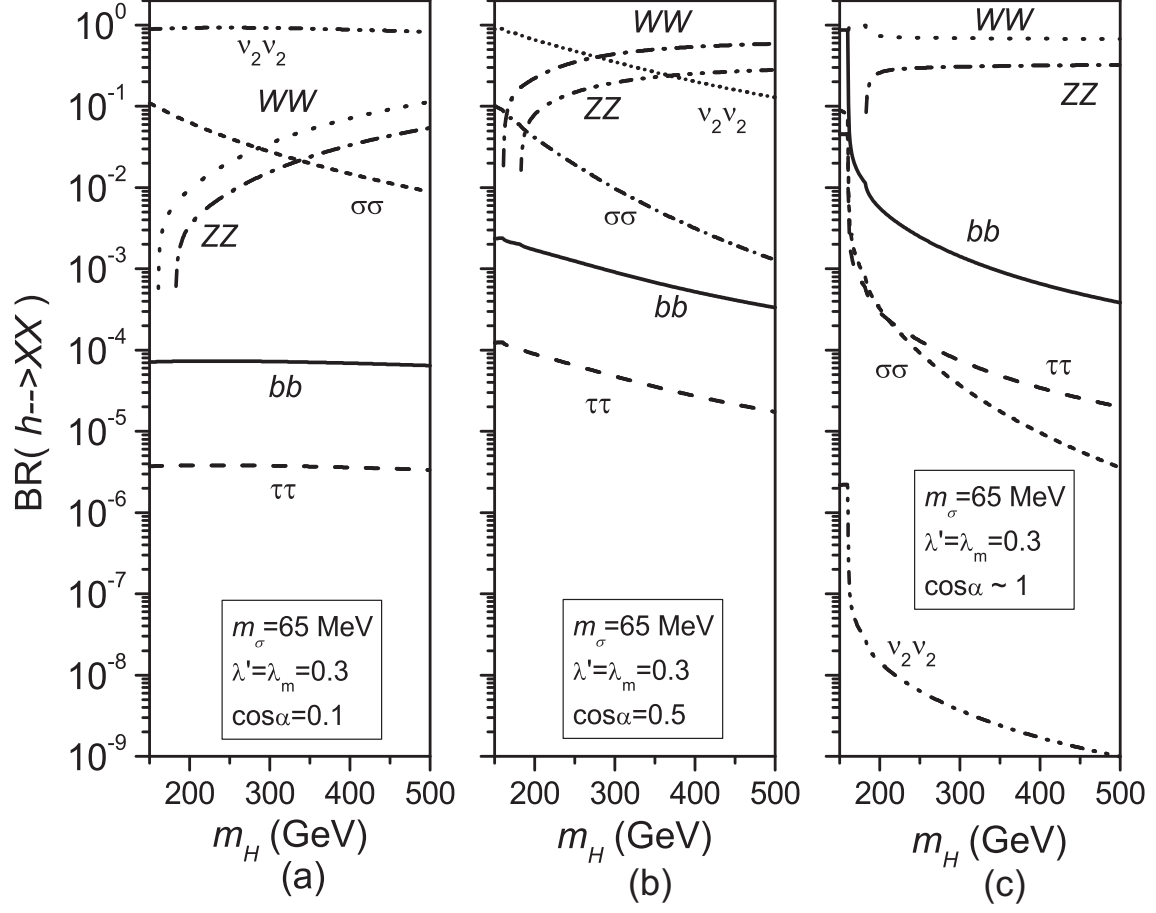
FIG. 10: Braching ratios for the decay $H \to XX$ with $m_\sigma = 65\,\text{MeV}$, $\lambda' = \lambda_m = 0.3$ and three different values for $\cos\alpha$: (a) $\cos\alpha = 0.1$, (b) $\cos\alpha = 0.5$ and (c) $\cos\alpha \approx 1$.